Atomic resolution study of the interfacial bonding at $Si_3N_4/CeO_{2-\delta}$ grain boundaries

W. Walkosz,[1] R. F. Klie,[1,a)] S. Öğüt,[1] A. Borisevich,[2] P. F. Becher,[2] S. J. Pennycook,[2] and J. C. Idrobo[1,2,3]

[1]*Department of Physics, University of Illinois at Chicago, Chicago, Illinois 60607, USA*
[2]*Oak Ridge National Laboratory, Materials Science and Technology Division, P.O. Box 2008, Oak Ridge, Tennessee 37831-6030, USA*
[3]*Department of Physics, Vanderbilt University, Nashville, Tennessee 37235, USA*

(Received 14 May 2008; accepted 18 July 2008; published online 6 August 2008)

Using a combination of atomic-resolution *Z*-contrast imaging and electron energy-loss spectroscopy (EELS) in the scanning transmission electron microscope, we examine the atomic and electronic structures at the interface between Si_3N_4 $(10\bar{1}0)$ and CeO_{2-d} intergranular film (IGF). Ce atoms are observed to segregate to the interface in a two-layer periodic arrangement, which is significantly different from the structure observed in a previous study. Our EELS experiments show (i) oxygen in direct contact with the terminating Si_3N_4 open-ring structures, (ii) a change in the Ce valence from a nominal oxidation state of +3 to almost +4 moving from the interface into the IGF, and (iii) a uniform concentration of Si in the film. © *2008 American Institute of Physics*.
[DOI: 10.1063/1.2968683]

Silicon nitride ceramics have desirable physical and mechanical properties in many high temperature and pressure applications. The wide-spread use of Si_3N_4 as a structural component is, however, limited by its brittleness.[1] Rare-earth oxides (REOs), when included as sintering additives, have long been known to overcome this problem by forming an intergranular film (IGF). The resulting microstructure has been shown to control the mechanical properties of Si_3N_4.[2] Until a few years ago, atomic scale information about the bonding characteristics at Si_3N_4/REO interfaces was lacking. The understanding of the toughening mechanism was largely empirical. Recent scanning transmission electron microscopy studies have demonstrated that the structure of the IGF formed by REOs is partially ordered, with the rare-earth elements arranged periodically at the Si_3N_4/IGF interface.[3–5] The various bonding patterns of the RE elements were correlated with their atomic radii, the electronic configuration, and the presence of oxygen at the interface.[4]

A detailed understanding of the atomic arrangements at Si_3N_4/REO interfaces and their implications for the Si_3N_4 mechanical properties requires investigations of the electronic structure, which can be achieved experimentally by atomic-resolution electron energy-loss spectroscopy[6] (EELS) in combination with *Z*-contrast imaging.[7] Although many Si_3N_4/REO interfacial structures have been imaged in recent experiments, to date, one atomic-resolution EELS study was performed for the Si_3N_4/Sm_2O_3 interface.[4] Another more recent paper examined Si_3N_4/IGF interfaces in Gd-doped Si_3N_4.[8] The Si_3N_4/Sm_2O_3 study, while providing useful information about the REO electronic structure, gave only *indirect* evidence for the presence of interfacial oxygen. The study of Si_3N_4/Gd-based IGF examined the effects of electron irradiation on the stability of the interfacial Gd adsorption sites using *Z*-contrast imaging and EELS. Neither of these earlier studies addresses the valence states of the RE elements, which are important for elucidating local electronic environments. Cerium, for example, has a well-known ability to change its valence state under different local oxygen environments.[9] Motivated by these observations, in this letter, we report a study of the interface between the Si_3N_4 $(10\bar{1}0)$ surface and the $CeO_{2-\delta}$ IGF using atomic-resolution *Z*-contrast imaging and EELS. Our EELS experiments show that oxygen is present at the interface in direct contact with the terminating Si_3N_4 open rings. We also show that the Ce valence state changes from +3 to almost +4 from the Si_3N_4 grain into the IGF. Finally, our analysis indicates that the N concentration decreases in going from the Si_3N_4 grain to the IGF, while the Si concentration remains unchanged.

The polycrystalline sample was synthesized from the powder mixture of Ube E-10 Si_3N_4 (Ub Industries, Ltd., Tokyo) with an additive composition of 8 wt % $CeO_{2-\delta}$ and 2 wt % MgO (Alfa Aesar, Ward Hill, MA) (see Ref. 10 for more details). The experimental *Z*-contrast images and EELS spectra were acquired with the UIC-JEOL2010F microscope at the University of Illinois at Chicago, resulting in a probe size of 1.4 Å for *Z*-contrast imaging and 1.6 Å probe for EELS with an energy resolution of 1.0 eV.

Figure 1 shows the atomic-resolution *Z*-contrast image of two Si_3N_4 grains separated by a ceria IGF with an average width of 1.2 ± 0.3 nm. The Si_3N_4 crystal structure forms characteristic hexagonal rings in the [0001] orientation exhibiting open-ring structures along $[0\bar{1}0]$ in the terminating plane, which can be identified in the image. The bright band above the Si_3N_4 *c*-axis oriented grain is the IGF with three distinctive Ce atomic columns periodically arranged in two layers. In the first layer, which is in direct contact with the [0001] oriented Si_3N_4 grain, Ce atoms segregate to the middle (B) and the end of the open rings (A). In the second layer they sit in between the open rings (C). While the present *Z*-contrast images indicate a two-layer periodic arrangement of Ce atoms, similar to the structure observed by Ziegler *et al.*,[11] there are significant differences between the

a)Author to whom correspondence should be addressed. Electronic mail: rfklie@uic.edu.

 © 2008 American Institute of Physics

Downloaded 23 Feb 2009 to 160.91.159.246. Redistribution subject to AIP license or copyright; see http://apl.aip.org/apl/copyright.jsp

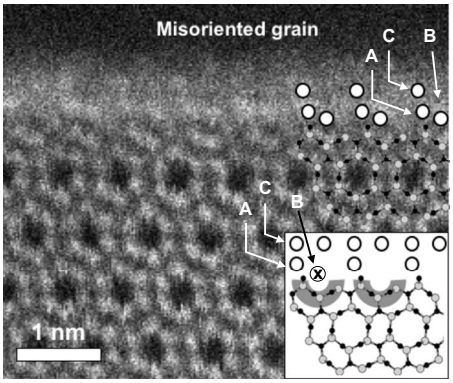

FIG. 1. High-resolution *Z*-contrast image of the Si_3N_4 $(10\bar{1}0)$ interface with the $CeO_{2-\delta}$ IGF. The Ce atoms (circled) in the nominally amorphous IGF are visible as bright contrast spots. The superimposed atomic structure shows Si and N atoms with light and dark circles, respectively. The actual arrangement of N atoms at the interface shown bonded with Si atoms in the schematic may differ when oxygen is present at the interface. The insert shows a schematic representation of the interfacial structure as found in the study by Ziegler *et al.* (see Ref. 11).

Ce positions in the two studies (Fig. 1). In particular, the main difference between the structure observed by Ziegler *et al.*[11] and the one reported here is the presence of Ce atoms at B. We observe that the Ce atoms attach at the middle of the open rings (B), as previously reported for Sm,[4] La,[5] and Gd (Ref. 12) based IGFs, whereas Ziegler *et al.*[11] observed this site to be vacant. Since the surface termination of this grain is identical in the two studies, we speculate that this structure variation can be attributed to the different local cations and oxygen environments surrounding the Ce atoms. The La, Gd, Sm, and our ceria based IGF were prepared with 2 wt % MgO, while the sample of Ziegler *et al.*[11] incorporated 1 wt % Al_2O_3. We also find a slight difference in the position of the Ce atoms (C) in the second layer with respect to observation of Ziegler *et al.*[11]

In our EELS analysis of an equivalent $Si_3N_4/IGF/Si_3N_4$ interface, we obtained spectra containing both the O and Ce core-loss signals acquired simultaneously. The spacing between each recorded spectrum is 1.0 Å. Figure 2(a) shows the background subtracted oxygen *K*-edges at 532 eV and the cerium *M*-edges at 880 eV as a function of the electron probe position across the interface. We find a clear signal of the O

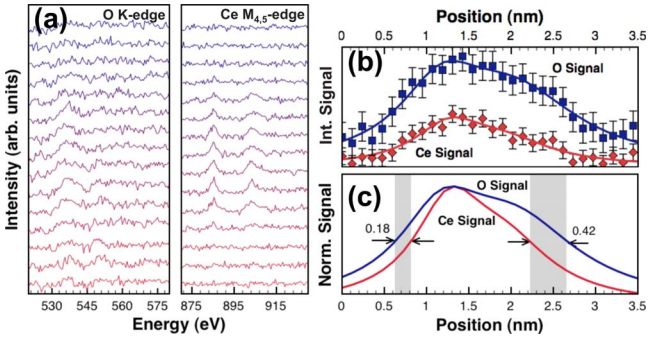

FIG. 2. (Color online) (a) EELS line scan after background subtraction showing the O *K*-edge and the Ce *M*-edge as a function of position across the IGF. Only one out of every second spectrum is shown for visualization purposes. (b) O *K*-edge and Ce *M*-edge signals integrated over 50 eV windows and fitted to a model with two Gaussians (solid lines) as a function of position across the film. The error bars indicate the standard error of the concentration quantification. (c) Normalized O and Ce signal fits.

K-edge and Ce *M*-edge coming from the IGF, although the former exhibits a lower signal-to-noise ratio than the latter. Figure 2(b) shows the O and Ce signals integrated over 50 eV windows starting at their respective edge-onsets. A nonlinear fit using a model with two Gaussians for the integrated O and Ce signals reveals that the full width at half maximum (FWHM) of the O signal is 0.60 nm wider than that of the Ce signal [see Fig. 2(c)]. Moreover, the onset of the O signal occurs 0.18 nm before the Ce signal at the interface between the Si_3N_4 open-ring surface and the IGF, strongly suggesting that the Si_3N_4 open rings can also be oxygen terminated.[13] This view is also supported by the earlier findings of Ziegler *et al.*[4] and our recent first-principles calculations for the bonding sites and structural energetics of oxygen at the Si_3N_4 $(10\bar{1}0)$ surface.[14] We find that for a wide range of surface coverage, oxygen always binds to Si for the lowest-energy configurations, typically bridging two Si atoms (Si–O–Si) much like the atomic configuration in SiO_2. In Fig. 2(b), we also notice that the integrated signal across the IGF does not have a symmetric profile. For instance, the Ce signal has a larger intensity at the interface with the Si_3N_4 open-ring structure [left hand side of Fig. 2(b)]. This effect is most likely the result of a sharper projection of the [0001] oriented grain compared to the misoriented grain. Moreover, this effect is also observed in the O signal, as would be expected if they were in direct contact with the open-ring surface of the [0001] oriented grain.

In a subsequent experiment, we obtained the Ce *M*-edges to determine the Ce valence and its spatial variation. Figure 3(a) shows Ce $M_{4,5}$-edge intensities and edge onset for spectra taken at the center of the film and at the interface with the Si_3N_4 grain. It can be clearly seen that the M_4/M_5 intensity ratio and the onset energy are lower in the middle of the IGF compared to the interface. These two quantities have been shown to be related to the Ce valence state,[15] as presented by the reference spectra in the insert of Fig. 3. Comparing the M_4/M_5 ratio and the chemical shift of the reference spectra with our experimental results, we find that the valence state of Ce is close to Ce^{3+} at the interface, and close to Ce^{4+} in the middle of the IGF. This result shows that ceria and reduced ceria can be found within the IGF due to different local oxygen concentration across the IGF.

Figure 3(b) shows Si and N concentration profiles across two Si_3N_4 grains with the ceria IGF in between. It can be seen that the N concentration decreases significantly when going across the Si_3N_4/CeO_2 interface, but the Si concentration remains nearly constant throughout the whole IGF. This finding has not been addressed in the existing literature, and has potentially important implications for future theoretical models.

In summary, using a combination of atomic-resolution *Z*-contrast imaging and EELS, we have observed that Ce atoms form a two-layer periodic arrangement at the $Si_3N_4/CeO_{2-\delta}$ interface, the details of which are affected most likely by the sintering additives. Our experiments show that the Si concentration is constant across the whole width of the IGF, while the N concentration decreases and the O concentration increases in the film. We also find that the onset of the O signal occurs ~0.18 nm before the Ce signal at the interface between the Si_3N_4 open-ring surface and the IGF, which combined with our first-principles calculations strongly suggests the Si_3N_4 open rings can also be oxygen

Downloaded 23 Feb 2009 to 160.91.159.246. Redistribution subject to AIP license or copyright; see http://apl.aip.org/apl/copyright.jsp

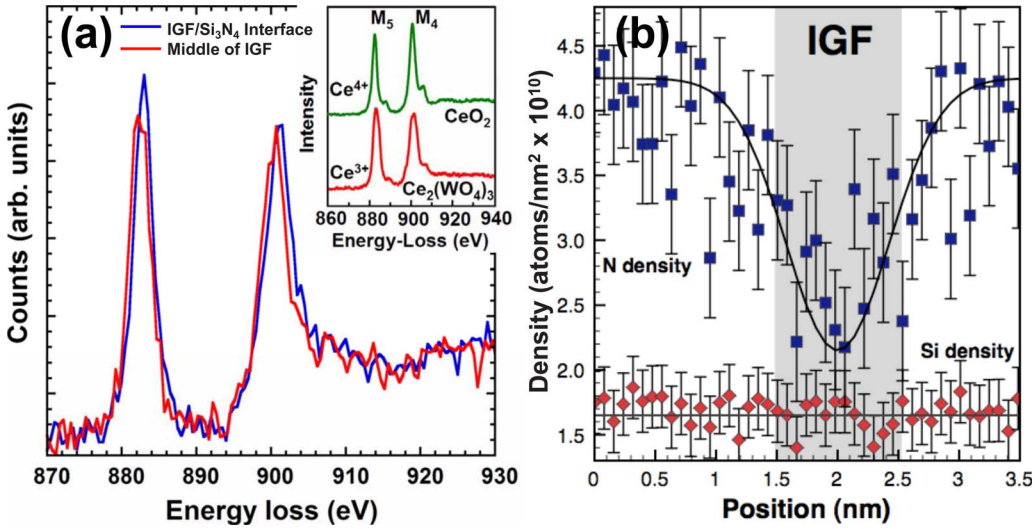

FIG. 3. (Color online) (a) Near edge fine-structure of the Ce *M*-edge taken from the middle and at the interface of the Si_3N_4/IGF. The insert shows reference spectra (from Ref. 14) obtained for CeO_2 and $Ce_2(WO_4)_3$, corresponding to valences of Ce^{4+} and Ce^{3+}, respectively. (b) Si and N concentration profiles across the $Si_3N_4/CeO_{2-\delta}$ interface extracted from an EELS line scan. The Si *L*-edge and the N *K*-edge were background subtracted, integrated over a 40 eV window, and multiplied by the corresponding scattering cross sections. The error bars indicate the standard error of the concentration quantification.

terminated. Furthermore, we have shown that the Ce valence changes across the IGF from +3 at the interface to almost +4 inside the IGF.

This work was supported by the NSF under Grant No. DMR-0604964 (W.W., S.O., and J.C.I.) and by the Division of Materials Sciences and Engineering, U.S. DOE under contract with UT-Battelle (A.B., P.F.B., and S.J.P.).

[1] *Materials Science and Technology, Structure and Properties of Ceramics*, edited by R. W. Cahn, P. Hassen, and E. J. Kramer (Wiley, Weinheim, 1994), Vol. 11, pp. 402 and 751.
[2] E. Y. Sun, P. F. Becher, K. P. Plucknett, C. H. Hsueh, K. B. Alexander, S. B. Waters, K. Hirao, and M. E. Brito, J. Am. Ceram. Soc. **81**, 2831 (1998); R. L. Satet and M. J. Hoffmann, J. Eur. Ceram. Soc. **24**, 3437 (2004).
[3] N. Shibata, S. J. Pennycook, T. R. Gosnell, G. S. Painter, W. A. Shelton, and P. F. Becher, Nature (London) **428**, 730 (2004).
[4] A. Ziegler, J. C. Idrobo, M. K. Cinibulk, C. Kisielowski, N. D. Browning, and R. O. Ritchie, Science **306**, 1768 (2004).
[5] G. B. Winkelman, C. Dwyer, T. S. Hudson, D. Nguyen-Manh, M. Doblinger, R. L. Satet, M. J. Hoffmann, and D. J. H. Cockayne, Philos. Mag. Lett. **84**, 755 (2004).
[6] R. F. Egerton, *Electron Energy Loss Spectroscopy in the Electron Microscope*, 2nd ed. (Plenum, New York, 1986).
[7] S. J. Pennycook and L. A. Boatner, Nature (London) **336**, 565 (1988).
[8] K. van Benthem, G. S. Painter, F. W. Averill, S. J. Pennycook, and P. F. Becher, Appl. Phys. Lett. **92**, 163110 (2008).
[9] N. V. Skorodumova, S. I. Simak, B. I. Lundqvist, I. A. Abrikosov, and B. Johansson, Phys. Rev. Lett. **89**, 166601 (2002); F. Esch, S. Fabris, L. Zhou, T. Montini, C. Africh, P. Fornasiero, G. Comelli, and R. Rosei, Science **309**, 752 (2005).
[10] P. F. Becher G. S. Painer, N. Shibata, S. B. Waters, and H.-T. Lin, J. Am. Ceram. Soc. **91**, 2328 (2008).
[11] A. Ziegler, J. C. Idrobo, M. K. Cinibulk, C. Kisielowski, N. D. Browning, and R. O. Ritchie, Appl. Phys. Lett. **88**, 041919 (2006).
[12] N. Shibata, G. S. Painer, R. L. Satet, M. J. Hoffmann, S. J. Pennycook, and P. F. Becher, Phys. Rev. B **72**, 140101(R) (2005).
[13] Removing the oxygen background before normalizing the O signal does not change the conclusions. The O FWHM is 0.46 nm broader than that of the Ce signal. The onset of the O signal occurs 0.1 nm before the Ce signal.
[14] W. Walkosz, J. C. Idrobo, R. F. Klie, and S. Öğüt (unpublished).
[15] L. J. Wu, H. J. Wiesmann, A. R. Moodenbaugh, R. F. Klie, Y. Zhu, D. O. Welch, and M. Suenaga, Phys. Rev. B **69**, 125415 (2004).

Downloaded 23 Feb 2009 to 160.91.159.246. Redistribution subject to AIP license or copyright; see http://apl.aip.org/apl/copyright.jsp